DC–DC Converters Dynamic Modeling With State Observer-Based Parameter Estimation

Hugues Renaudineau, Jean-Philippe Martin, Babak Nahid-Mobarakeh, *Senior Member, IEEE*, and Serge Pierfederici

***Abstract*—Online knowledge of dc–dc converters behavior is always of great interest. Based on a reliable model of the converters, some great improvement can be achieved. First, the control of the converters can be designed more precisely, especially while thinking in nonlinear theories model-based controls, and it can help to improve the energy management and the efficiency. Also, the knowledge of the converters gives some really useful indications about their state of health and, then, represents a good diagnosis tool and fault detection possibility. This paper proposes a modeling of the converters and a new state observer dedicated to an online estimation of the model parameters. The proposed average models include parameter modeling the losses and their estimation. They are validated on two different converters: the classical dc–dc boost converter and the current-fed dual-bridge dc–dc converter (CFDB—also called isolated boost). It is shown that the model of this last converter is strongly nonlinear, which impacts on the estimation. Simulations and experimental validation are given both on the boost and the isolated boost, and comparisons with the Luenberger state observer and extended Kalman filter are given to underline the interest of the proposed parameter estimation in terms of convergence for nonlinear systems and convergence rapidity.**

***Index Terms*—Current-fed dual-bridge (CFDB) dc–dc converter, dc–dc boost converter, online parameter estimation, state observer.**

I. Introduction

DC–DC converters are widely used among power electronics applications any time dc electrical power requires to be converted from a given level to another [1]. Online knowledge of their behavior is always of great interest [2]. Based on a reliable dynamic model of the converters, some great improvements can be achieved.

1) The control of the converters can be designed more precisely. For examples, model-based control techniques are proposed in [3]–[5] with applications on dc–dc converters. Other control methods require the knowledge of the converter model, especially nonlinear theory model-based control techniques such as flatness-based controls as used in [6].
2) It can be used to improve the energy management as done in [7], where a model-based current sharing for the parallel structure is proposed for efficiency improvement.
3) It gives some really useful indications about their state of health and, then, represents a good diagnosis tool and fault detection possibility as proposed in [8].

Manuscript received November 23, 2013; revised April 28, 2014; accepted June 24, 2014. Date of publication July 8, 2014; date of current version January 16, 2015. Recommended for publication by Associate Editor J. Clare.

The authors are with the Research Group in Electrical and Electronics, Université de Lorraine, 54518 Vandoeuvre-les-Nancy, France (e-mail: hugues.renaudineau@univ-lorraine.fr; jean-philippe.martin@univ-lorraine.fr; babak.nahidmobarakeh@univ-lorraine.fr; serge.pierfederici@univ-lorraine.fr).

Color versions of one or more of the figures in this paper are available online at http://ieeexplore.ieee.org.

Digital Object Identifier 10.1109/TPEL.2014.2334363

DC–DC converters modeling has been largely tackled along the literature but is still under study as for recent example in [9]. Many improvements on the converters modeling can be found. Among them, in [10] it is proposed to calculate losses are predicted from analytic model. Also, in [11], some algebraic parameter estimation for improving the control of a boost converter is proposed. Other parameter estimation method is proposed in [12], with sampling frequency equal to twice the switching frequency, and estimated parameters are used to improve converter control in [13]. In this paper, the proposed modeling and estimation have been designed for a sampling frequency equal to the switching frequency, and then, only the average values of the state variables can be measured. Then, the average model of the converter is considered. In this way, particular attention has been given to the model and estimation method proposed in [14] on the case of a boost converter.

This paper proposes a modeling of the converters and a state observer dedicated to an online estimation of the model parameters. State observers can be used for fault detection as for example in [8]. State observers also have been applied to parameter estimation on dc–dc converters. For example, in [15], Al-Hosani and Utkin introduced a sliding mode observer to estimate the output capacitor and the equivalent resistive load on a dc–dc buck converter. Kalman filter method is another widely used solution in industrial applications [16], which can either be used for parameter estimation or fault diagnosis. In [17], Izadian and Khayyer use a Kalman filter for fault diagnosis on a dc–dc boost converter based on a time-averaging model, by comparing the system with multiple models representing fault signatures. In this paper, to underline the interest of the proposed state observer dedicated to parameter estimation, comparisons with Luenberger state observer and an extended Kalman filter (EKF) are provided.

Simulations and experimental validation are given both on the classical dc–dc boost converter and the current-fed dual-bridge (CFDB) dc–dc converter also called isolated boost converter. Still, the proposed modeling approach and estimation can be easily adapted to other dc–dc conversion structures, such as buck, buck–boost, etc.

Before a conclusion summarizing the main contributions of this proposal, this paper is organized as follows. First, Section II presents the average dynamical model applied on a boost converter and an isolated boost converter. Then, Section III gives the definition of the proposed state observer, with demonstration on

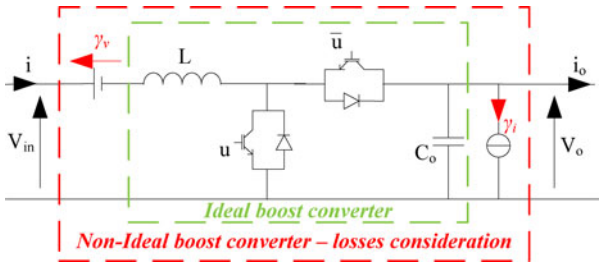

Fig. 1. Boost converter—Equivalent circuit-type model.

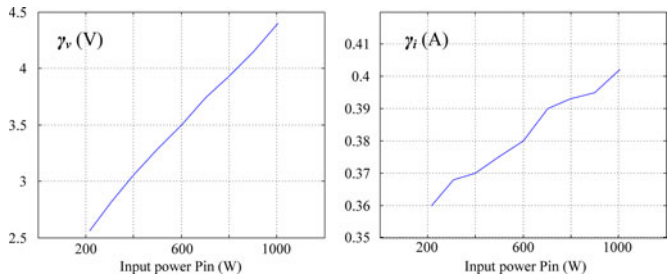

Fig. 2. Losses parameters evolution with respect to the input power P_{in}—Experimental estimation on a boost converter.

its convergence. Finally, Sections IV and V give simulations and experimental validation, respectively, on the boost converter and the isolated boost converter with comparisons with Luenberger state observer and EKF.

II. DC–DC Converters Modeling

A. Boost Converter

Based on the ideal model, some modifications are proposed to include internal losses of the converter in the model. It is proposed to model average values of the state variable of the boost converter as (1a) and (1b) in which average value of the variable x is notated as $\bar{x}$. Equivalent circuit of the proposed model is represented as in Fig. 1

$$\begin{cases} L\dfrac{d\bar{i}}{dt} = V_{\text{in}} - (1-d)\bar{V}_o - \gamma_v & \text{(1a)} \\ C_o\dfrac{d\bar{V}_o}{dt} = (1-d)\bar{i} - i_o - \gamma_i. & \text{(1b)} \end{cases}$$

Parameters $\gamma_v(V)$ and $\gamma_i(A)$ counterbalance the errors with the ideal model of the boost converter. Then, those parameters directly traduce the internal losses of the converter. Principal losses which are taken into account are inductance series resistance, core hysteresis and eddy current losses, conduction ohmic losses, and switching losses of semiconductors. Every other losses through the converter are also taken into account. The equivalent losses parameters γ_v and γ_i vary with respect to the functioning point. Fig. 2 shows their evolution with respect to the power in the case of a 48–100 V boost converter. Results presented in this figure have been obtained experimentally with the estimation method detailed in Section III. Finally, an online dynamic-efficient estimation of those parameters is of real interest in order to have the most precise model as possible.

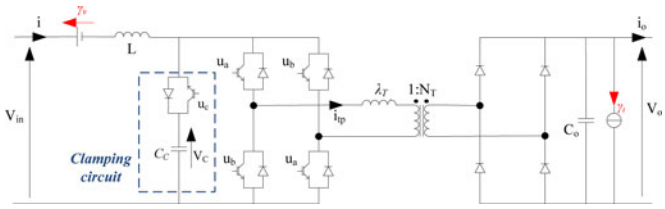

Fig. 3. Isolated boost converter with the clamping circuit.

B. Isolated Boost Converter

As the used reduced-order average model of the isolated boost converter is less common, some details on its obtaining and validation are given. Still, leading ideas can be found in [18], and a detailed validation of this model is given in [2].

The isolated boost converter requires some additional circuit for starting as underlined in [19] and [20]. In this paper, the converter is supposed to operate in boost mode, then verifying

$$\bar{V}_o \geq N_t V_{\text{in}}. \tag{2}$$

The dead-time effect as studied in [21] is neglected. Also, it is supposed that the magnetization inductance is enough important to neglect the magnetization current. On the other hand, the influence of the leakage of the transformer is taken into account. Because of the leakage of the transformer, an additional clamping circuit must be considered to reduce overvoltage across the switches [20], [22]. The isolated boost with the clamping circuit considered in this paper is represented in Fig. 3 with associated notations. As for the boost converter, a voltage source and current source $\gamma_v(V)$ and $\gamma_i(A)$ are added in the equations to model the losses of the converter.

To determine an average dynamical model of the isolated boost converter, ideal waveform of the transformer current is considered as represented in Fig. 4, and an energetic analysis is realized. In Fig. 4, it can indeed be viewed that current i_{tp} is discontinuous since magnetization of the transformer is neglected.

First, the transformer primary current maximum value can be calculated through (3) since its slope is known on sequence $S2$ whose duration is known

$$i_{\text{tp}_{\max}} = \frac{1}{\lambda_T}\left(\bar{V}_C - \frac{\bar{V}_o}{N_T}\right)(1-2d)\frac{T}{2}. \tag{3}$$

Then, the duration of the sequence $S0$ can also been calculated through (4). For this, attention focuses on the sequence between $T/2$ and $T/2+\beta T$, where the transformer primary current i_{tp} decreases from $i_{\text{tp}_{\max}}$ to 0 with a constant slope

$$\beta = \frac{\lambda_T}{T}\frac{i_{\text{tp}_{\max}}}{\frac{\bar{V}_o}{N_T}}. \tag{4}$$

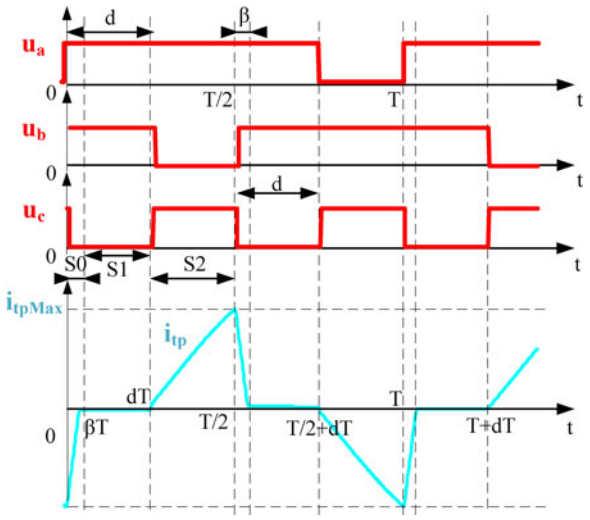

Fig. 4. Waveform of the transformer primary current i_{tp}.

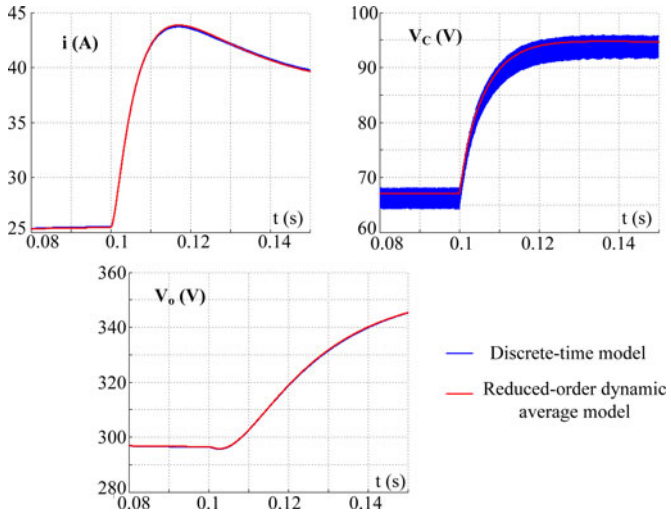

Fig. 5. Simulation of the reduce-order average model—Response for a step of duty cycle in open loop.

Also, the derivatives of the average values of the voltages $\bar{V}_C$ and $\bar{V}_o$ can be expressed as follows:

$$C_c \frac{d\bar{V}_c}{dt} = (1-2d)\,\bar{i} - (1-2d)\,\frac{i_{\mathrm{tp_{max}}}}{2} \tag{5}$$

$$C_o \frac{d\bar{V}_o}{dt} = -i_o + \frac{1}{2N_T} i_{\mathrm{tp_{max}}}\,(1-2d+2\beta)\,. \tag{6}$$

Finally, losses parameters γ_v and γ_i are introduced in the modeling, and a reduce-order dynamic model is proposed following (7a)–(7c)

$$\begin{cases} L\dfrac{d\bar{i}}{dt} = V_{\mathrm{in}} - (1-2d)\,\bar{V}_C - \gamma_v & \text{(7a)} \\ C_C \dfrac{d\bar{V}_C}{dt} = (1-2d)\,\bar{i} - (1-2d)^2\,\dfrac{T}{4\lambda_T}\left(\bar{V}_C - \dfrac{\bar{V}_o}{N_T}\right) & \text{(7b)} \\ C_o \dfrac{d\bar{V}_o}{dt} = (1-2d)^2\,\dfrac{T}{4\lambda_T}\left(\bar{V}_C - \dfrac{\bar{V}_o}{N_T}\right) \\ \qquad \times \left[\dfrac{1}{N_T} + \dfrac{\left(\bar{V}_C - \frac{\bar{V}_o}{N_T}\right)}{\bar{V}_o}\right] - i_o - \gamma_i & \text{(7c)} \end{cases}$$

The validity of the proposed reduce-order average dynamic model has been verified through simulation. Fig. 5 attests the validity of the proposed reduce-order average dynamic model. Indeed, it can be seen in this figure that this model does efficiently model the average value of the state variables. For this simulation, the isolated boost converter is in open loop, and a step on the duty cycle is applied at time $t = 0.1$ s. The converter is connected to a resistive load $R_{\mathrm{Load}} = 80\ \Omega$.

III. State Observer for Parameter Estimation

In this section, a new state observer is proposed. This state observer, is dedicated to a specific subclass of nonlinear systems. It will be demonstrated that for observable systems, estimated variables converge exponentially to actual ones with the proposed state observer. The proposed state observer inspires from the subclass of state observers designated through the literature as "disturbance observers" as studied for example in [23] and [24]. Disturbance observers are indeed very well adapted to the considered problematic consisting in losses estimation. Indeed, especially on the case of the boost converter, if considering $\mathrm{disturb} = (\gamma_V \quad \gamma_I)^T$, the disturbance observers are well adapted. Furthermore, losses can be interpreted as disturbance compared to ideal. Still, the main difference with the disturbance observer comes from the fact that with the proposed state observer, it is possible to estimate parameters, which are linked to the state variables of the model (i.e., with $g(x,u)$ defined in (8) different from identity).

A. Considered System

The proposed state observer is dedicated to the subclass of nonlinear systems which can be described as follows:

$$\begin{cases} \dot{X} = \begin{pmatrix} \dot{x} \\ \dot{p} \end{pmatrix} = \begin{pmatrix} f(x,u) + g(x,u)\cdot p \\ 0 \end{pmatrix} \\ Y = x \end{cases} \tag{8}$$

where:

1) $X \in \Re^{n+m}$ is the vector of variable which is going to be estimated, and $Y \in \Re^n$ is the vector of measured variables;
2) $x \in \Re^n$ is the vector of the system state variables. Every state variable is supposed to be measured (i.e., $Y = x$);
3) $p \in \Re^m$ is the vector of the unknown parameters to estimate. Parameters p are supposed to vary slowly compared to state variables (i.e., $|\dot{p}| \ll |\dot{x}|$);
4) f and g are nonlinear functions of x and u (the command signal vector), respectively, of size $\Re^n$ and $\Re^{n\times m}$.

B. State Observer Definition

For the subclass of nonlinear systems verifying (8), the proposed state observer is defined through (9), considering the

estimation errors $\varepsilon_x = (\hat{x} - x)$ and $\varepsilon_p = (\hat{p} - p)$

$$\begin{pmatrix} \dot{\hat{x}} \\ \dot{\hat{p}} \end{pmatrix} = \begin{pmatrix} f(x,u) + g(x,u)\cdot\hat{p} - S\cdot\varepsilon_x \\ K_p\cdot\dot{\varepsilon}_x + K_i\cdot\varepsilon_x - g^T(x,u)\cdot\varepsilon_x \end{pmatrix} \tag{9}$$

with:

1) S positive-definite matrix of size $\Re^{n\times n}$;
2) P positive-definite matrix of size $\Re^{m\times m}$

and

$$\begin{cases} K_p\cdot g(x,u) = -P & \text{(10a)} \\ K_i = K_p\cdot S. & \text{(10b)} \end{cases}$$

For the calculation of parameters K_p and K_i as defined through (10a) and (10b), the inverse of matrix $g(x,u)$ is required. In the case $g(x,u)$ is square (i.e., $n = m$) and nonsingular, the inverse can be used. More generally (if g is singular or rectangular), parameter K_p is calculated by considering a pseudoinverse of $g(x,u)$. The theory on pseudoinverse can be found in [25]. It can be noticed that the result of the pseudoinverse is generally not unique, any of the solutions being suitable for the calculation of parameter K_p. This degree of freedom can be used to make easy the calculation of the algorithm.

The proposed state observer has been designed in order to obtain a system for which the exponential stability can be proven. Especially, for the part of the system corresponding to the estimation of the parameters p—bottom of (9)—the terms $K_p\cdot\dot{\varepsilon}_x$ and $K_i\cdot\varepsilon_x$ have been added in order to verify the exponential stability. Indeed without those terms (i.e., only considering $\dot{\hat{p}} = -g^T(x,u)\cdot\varepsilon_x$), only the asymptotic stability can be demonstrated.

C. Stability of the Estimation

For demonstrating the convergence of the estimation through the state observer, the derivative estimation errors ε_x and ε_p are written, respectively, as follows:

$$\dot{\varepsilon}_x = g(x,u)\cdot\varepsilon_p - S\varepsilon_x \tag{11}$$

$$\dot{\varepsilon}_p = K_p\cdot g(x,u)\cdot\varepsilon_p - K_p\cdot S\cdot\varepsilon_x + K_i\cdot\varepsilon_x - g^T(x,u)\cdot\varepsilon_x. \tag{12}$$

Exponential stability of the estimation can be demonstrated with the classical Lyapunov approach. For this the Lyapunov candidate function, V is considered as follows:

$$V = \frac{1}{2}\cdot\begin{pmatrix}\varepsilon_x & \varepsilon_p\end{pmatrix}\cdot\begin{pmatrix}\varepsilon_x \\ \varepsilon_p\end{pmatrix} \geq 0. \tag{13}$$

The derivative of function V can be expressed as

$$\dot{V} = \varepsilon_x^T\cdot\dot{\varepsilon}_x + \varepsilon_p^T\cdot\dot{\varepsilon}_p. \tag{14}$$

By combining (11), (12), and (14), $\dot{V}$ can be expressed as

$$\begin{aligned}\dot{V} = {} & \varepsilon_x^T\cdot g(x,u)\cdot\varepsilon_p - \varepsilon_x^T\cdot S\cdot\varepsilon_x \\ & + \varepsilon_p^T\cdot K_p\cdot g(x,u)\cdot\varepsilon_p - \varepsilon_p^T\cdot K_p\cdot S\cdot\varepsilon_x \\ & + \varepsilon_p^T\cdot K_i\cdot\varepsilon_x - \varepsilon_p^T\cdot g^T(x,u)\cdot\varepsilon_x.\end{aligned} \tag{15}$$

Then, by introducing $K_p\cdot g(x,u) = -P$ and $K_i = K_p\cdot S$, it results

$$\dot{V} = \begin{pmatrix}\varepsilon_x & \varepsilon_p\end{pmatrix}\cdot\begin{pmatrix}-S & 0 \\ 0 & -P\end{pmatrix}\cdot\begin{pmatrix}\varepsilon_x \\ \varepsilon_p\end{pmatrix}. \tag{16}$$

From (13) and (16), the estimation exponentially stability can be ensured long as S and P are positive-definite matrix.

Finally, the tuning of the S and P matrices is based on the assumption that the dynamics of the state vector error ε_x have to be highly faster than the dynamics of the parameter vector error ε_p. This choice involves a design of the matrix S with eigenvalues real parts highly greater than those of P. To improve the convergence of the state vector error to zero (and in the case of the isolated boost converter, to take into account the effect of the clamp voltage on the current dynamic), coupling terms can be added.

IV. Validation on the Boost Converter

This section gives the validation of the proposed estimation method. The proposed state observer is compared with a Luenberger state observer and an EKF. To obtain a valuable comparison, parameters of each estimation method have been tuned experimentally to obtain the better performances.

A. Parameter Observability

Before presenting parameters γ_v and γ_i estimation, their observability must be verified, since it is proposed to estimate them through state observers. For this purpose, the considered state vector X follows:

$$X = \begin{pmatrix}\bar{i} & \bar{V}_o & \gamma_v & \gamma_i\end{pmatrix}^T. \tag{17}$$

Measured vector Y is as

$$Y = \begin{pmatrix}\bar{i} & \bar{V}_o\end{pmatrix}^T. \tag{18}$$

The observability of such a system can be proved considering the observability vector Θ

$$\Theta = \begin{pmatrix} Y \\ \dot{Y} \end{pmatrix} = \begin{pmatrix} X_1 \\ X_2 \\ \dfrac{1}{L}\left[V_{\text{in}} - X_3 - (1-u)X_2\right] \\ \dfrac{1}{C_o}\left[(1-u)X_1 - i_o - X_4\right] \end{pmatrix}. \tag{19}$$

In the considered case, (20) is verified if $X_1 = i \neq 0$. Then, the system is observable if the input power is different from 0 (not problematic since estimated parameters would not be used for null power)

$$\text{rank}\left(\text{Jacob}(\Theta)\right) = \dim(X) = 4. \tag{20}$$

B. Proposed State Observer Application

For developing the proposed state observer, the system is written in the form presented in Section III. Functions $f(x,u)$ and $g(x,u)$ follow (21) and (22). It is verified that $g(x,u)$ is

invertible

$$f(x,u) = \begin{pmatrix} \frac{1}{L}\left[V_{\text{in}} - (1-d)\bar{V}_o\right] \\ \frac{1}{C_o}\left[(1-d)\bar{i} - i_o\right] \end{pmatrix} \tag{21}$$

$$g(x,u) = \begin{pmatrix} -\frac{1}{L} & 0 \\ 0 & -\frac{1}{C_o} \end{pmatrix}. \tag{22}$$

To compete the proposed state observer, matrices S and P have to be determined. They are chosen as

$$S = \begin{pmatrix} 10\,000 & 0 \\ 0 & 10\,000 \end{pmatrix}, \quad P = \begin{pmatrix} 500 & 0 \\ 0 & 500 \end{pmatrix}. \tag{23}$$

C. Luenberger State Observer

As a comparison with the proposed state observer, a Luenberger state observer is designed. As it a state observer dedicated to linear systems, it is necessary to linearize the considered system around one operating point following (24). Variable u is in this case the command duty cycle d

$$\begin{cases} \dot{X} = A \cdot X + B \cdot u \\ Y = X. \end{cases} \tag{24}$$

The Luenberger state observer is then defined as (25)

$$\begin{aligned} \dot{\hat{X}} &= A\hat{X} + Bu - G(\hat{Y} - Y) \\ \dot{\hat{X}} &= A\hat{X} + Bu - \text{GC}(\hat{X} - X). \end{aligned} \tag{25}$$

The estimation will converge if the error $\tilde{X} = \hat{X} - X$ tends to 0. This will be realized if the matrix $(A - \text{GC})$ is stable, i.e., with eigenvalues with negative real part. In view of estimated values, we decide to impose two different convergence dynamics: a fast one for measured values (i and V_o), and a slower one for nonideal behavior parameters (γ_v and γ_i). This is realized by choosing value of the gain matrix G so that $(A - GC)$ eigenvalues approach $(-10^4 \quad -10^4 \quad -60 \quad -60)^T$. Those values have been tuned experimentally to obtain the better performances as possible. For the operating point: $i^0 = 5$ A, $V_{\text{in}} = 48$ V, $V_o^0 = 100$ V, $L = 0.6$ mH, $C_o = 1$ mF, and $d^0 = 0.52$, the matrix G allowing the proposed eigenvalues as follows:

$$G = 10^4 \begin{pmatrix} 0.9727 & 0 & 0 & -0.08 \\ 0.048 & 0.048 & 0.048 & 1.006 \\ 0 & 0 & -0.036 & 0 \\ 0 & 0 & 0 & -0.06 \end{pmatrix}. \tag{26}$$

For this estimation, even if the system has been linearized around one operating point, it has been experimentally verified that the estimation was converging in the power range 0–1 kW with no change of the value of the matrix G.

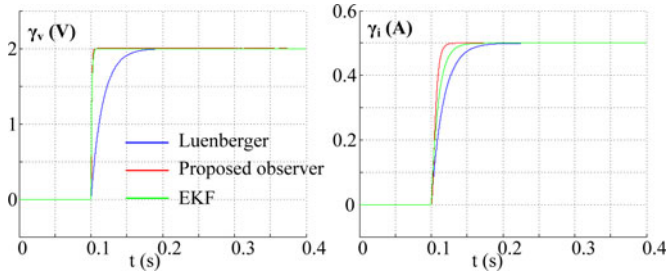

Fig. 6. Comparison between the different state observers.

D. Extended Kalman Filter

To develop the EKF, the system model is written as

$$\begin{cases} x_{k+1} = f(x_k, u_k) \\ y_k = h(x_k, u_k). \end{cases} \tag{27}$$

The EKF system is given by

$$\hat{x}_{k+1} = \hat{x}_{k+1/k} - K_{k+1}(h(\hat{x}_{k+1/k}, u_{k+1}) - y_{k+1}) \tag{28}$$

where

$$\begin{cases} \hat{x}_{k+1/k} = f(\hat{x}_k, u_k) \\ P_{k+1} = (I_n - K_{k+1}C_{k+1})\,P_{k+1/k} \\ P_{k+1/k} = A_k P_k A_k^t + Q_k \\ K_{k+1} = P_{k+1/k}C_{k+1}^t(C_{k+1}P_{k+1/k}C_{k+1}^t + R_{k+1})^{-1}. \end{cases}$$

The derivative matrix A_k and C_{k+1} are calculated following:

$$\begin{cases} A_k = \dfrac{\partial}{\partial x} f(\hat{x}_k, u_k) \\ C_{k+1} = \dfrac{\partial}{\partial x} h(\hat{x}_{k+1/k}, u_{k+1}). \end{cases}$$

The only things needed for completing the Kalman filter realization are its initial covariance matrix (P_0) and its weighting matrices (Q and R). Using a trial-and-error procedure, those parameters are set as

$$\begin{cases} P_0 = \text{diag}\left(10^4, 10^4, 60, 1000\right) \\ Q = \text{diag}\left(10^4, 10^4, 60, 1000\right) \\ R = \text{diag}\left(1, 1\right). \end{cases} \tag{29}$$

E. Simulation

Simulation has been realized to confirm the validity of the developed state observers and validate the interest of the proposed state observer. For this simulation, input voltage is $V_{\text{in}} = 48$ V, output voltage is regulated to 100 V and is connected to a resistive load $R_{\text{Load}} = 50\ \Omega$. For the simulation, cosimulation between a circuit-typed software and *Simulink* is used. It allows us to simulate the converter including detailed losses calculation in each components, while the control and estimation are realized under *Simulink*. Fig. 6 shows results from the different state observers. In this simulation, estimation is enabled at time $t = 0.1$ s.

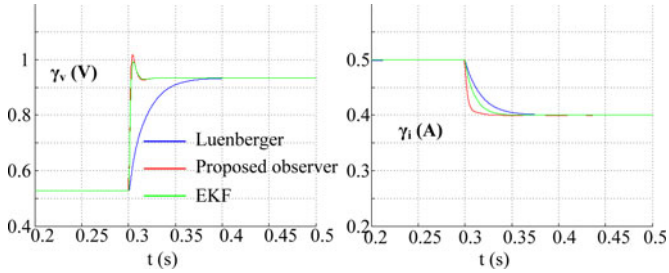

Fig. 7. Response of the estimation for a load step.

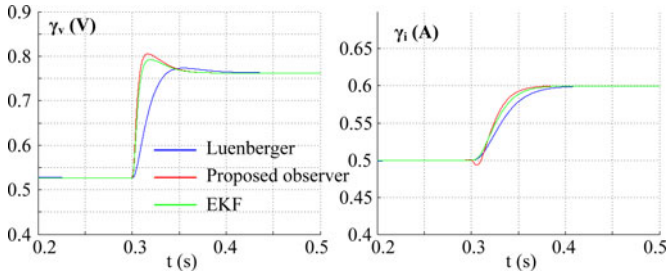

Fig. 8. Response of the estimation for step of V_o^{ref}.

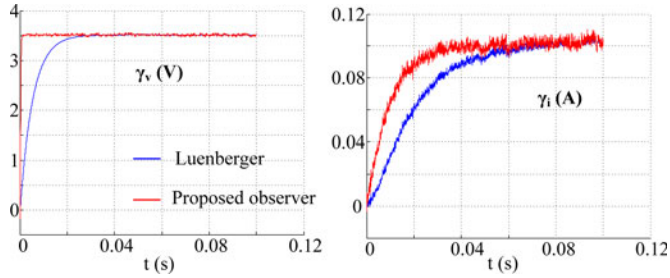

Fig. 9. Experimental verification of the estimation convergence.

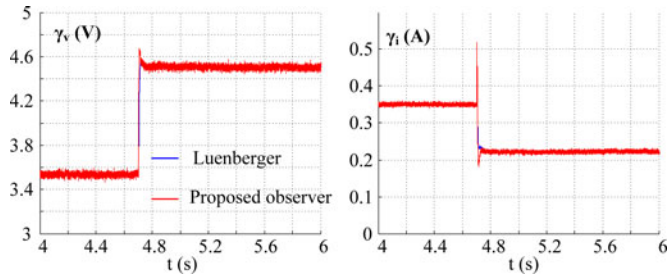

Fig. 10. Experimental behavior of the estimation for a load step.

In Fig. 6, the estimation is verified to converge to the desired values for each state observers. The fact that the estimated parameters converge to the simulated ones is important, since it will not be possible to verify it in the experiment as long as the estimated parameters corresponding to the losses are not physical elements and cannot be determined with another method, and then only the estimated efficiency can be compared with the measured one. Also, it can be observed that the Luenberger state observer is slower to converge, especially for parameter γ_v. The EFK and the proposed state observer converges in less than 50 ms with the chosen parameters, which have been experimentally adjusted to give a response as fast as possible.

The behavior of the estimated values has also been tested during transients. Fig. 7 shows the response of the estimated values for a load step at time $t = 0.3$ s from R_{Load} to $2R_{\mathrm{Load}}$. Fig. 8 shows response of the estimated values for a step on the regulated output voltage V_o^{ref} from 100 to 120 V at time $t = 0.3$ s.

In Figs. 7 and 8, it is verified that during transients, the estimated values change as expected, with convergence in a reasonable time.

F. Experiment

The behavior of the estimation has been experimented for validation. The dynamics of the three estimators have been experimentally tuned to obtain the good performances, in practice resulting in the previous mentioned parameters. First, it has been observed that even in practice where there is noise on measurement, the EKF does not give better results than the proposed state observer. Furthermore, estimation through EKF requires much more calculation capacity compared with the two other state observer. It explains well since the EKF has to invert matrix at any iteration which can be quite long. Computed on a dSpace 1103 device, overall calculation for control and estimation takes around 9 μs with Luenberger state observer method, 12 μs with the proposed state observer, and 29 μs with EKF. This large difference of required calculation time with no visible improvement on the result of estimation makes reject the EKF as a potential solution. Still, this solution can be adapted to others application especially if the noise on measurement increases (the EKF is well known to reject noise on measurement efficiently).

Fig. 9 shows the convergence of the proposed state observer estimation compared with Luenberger when estimation is enabled. As through simulations, it can be viewed in this figure that the proposed state observer is faster than the Luenberger state observer. Also, it has been verified that the estimated efficiency matches the measured one, so that it can be concluded that the estimation converges to the desired values.

The behavior of the estimated values has also been tested during transients as shown in Fig. 10 for a load step from 400 to 800 W. This result confirms the good behavior of the estimation under transient has shown through simulation.

V. Validation on the Isolated Boost Converter

For (7b) corresponding to the clamping capacitor voltage V_C, no additional parameter is added. This choice has been done so that it will be possible to estimate the value of the leakage inductance. This solution has been preferred since estimation convergence is very dependent on this parameter value. Similarly, the model is sensitive to errors on the transformer ratio N_T, but this last parameter can be more precisely known from the design of the transformer. Furthermore, the two parameters

cannot be estimated in the same time since the observability is not verified.

Then, it is proposed to estimate the vector X as

$$X = (\bar{i} \quad \bar{V}_C \quad \bar{V}_o \quad \gamma_V \quad \frac{T}{\lambda_T} \quad \gamma_I)^T. \tag{30}$$

The leakage inductance of the transformer is not directly estimated, but the ratio $\frac{T}{\lambda_T}$. This choice has been done not to have large dispersion between the value to estimate each value being scaled between 0.1 and 500. Indeed, if directly estimating the inductance value, the problem is that the matrices are numerically ill posed (amplitudes of largely different scales). This can pose problems in the estimation, and it is preferred to scale the values to estimate in a reasonable interval as done in [26] (the "scaled system" is designated as the "symmetric system" in [26]).

A. Parameter Observability

In the considered system, measurements are $Y = (\bar{i} \ \bar{V}_C \ \bar{V}_o)^T$. The Jacobian of the observability vector $\Theta = (Y \ \dot{Y})^T$. It has been verified that the rank of the Jacobian matrix is equal to the size of the estimated vector (i.e., $\text{rank}(\text{Jacob}(\Theta)) = \dim(X) = 6$). Then, the considered system is observable.

B. Parameter Estimation

As done with the boost converter, a Luenberger state observer has been designed. It results that this method is not suitable for this estimation which was diverging in the case of the isolated boost. This can be explained by a system to estimate which is much more nonlinear than the boost converter, and then, the required linearization for the Luenberger state observer design is a too restrictive hypothesis. Also, it has been experimentally verified that the design of a Kalman filter is really hard, since no suitable parameters have been found to ensure the estimation convergence.

To compete the proposed state observer, matrices S and P have been determined as follows:

$$S = \begin{pmatrix} 1000 & 1000 & 0 \\ 1000 & 10\,000 & 0 \\ 0 & 0 & 300 \end{pmatrix}$$

$$P = \begin{pmatrix} 500 & 0 & 0 \\ 0 & 500 & 0 \\ 0 & 0 & 500 \end{pmatrix}. \tag{31}$$

In matrix S, it can be underlined that a coupling term between measurement and estimation of the first two equations is used (no diagonal matrix). Once again, parameters have been tuned experimentally to obtain the better performances in practice.

C. Experiment

The design of the proposed state observer dedicated to parameter estimation on the isolated boost converter has also been tested experimentally. Fig. 11 attests the convergence of the estimation. As for the boost converter, it has been verified all along the experiment that the estimated converter efficiency converges to the measured one, then validating the estimation results.

It can be viewed in Fig. 11 that the parameters which allow estimating losses converge in a reasonable amount of time

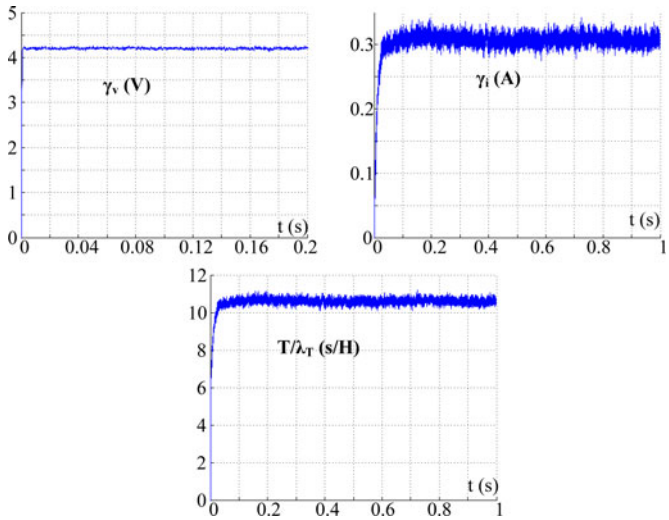

Fig. 11. Experimental estimation of the isolated boost parameters.

exactly as it was in the case of the boost converter. Furthermore, the third estimated parameter $\frac{T}{\lambda_T}$ is also converging, and it has been verified that its value was as expected. Indeed, the leakage inductance had previously been measured to be $\lambda_T = 5$ μH. Then, under a switching frequency of 20 kHz, the estimation of parameter $\frac{T}{\lambda_T}$ was expected to converge around 10 s/H. This is verified since estimation converges around 10.6 s/H, i.e., with an error of 5%.

For the parameter $\frac{T}{\lambda_T}$, it has been verified that the estimation was not depending on the functioning point with estimation results staying between 10.1 and 11.2 s/H on the interval 200–1000 W. Losses parameters γ_v and γ_i shown an evolution similar than in the case of the boost converter (see Fig. 2).

VI. Conclusion

This paper presented a modeling for dc–dc converters and a state observer dedicated to online estimation. The knowledge of the converter model is very useful for designing model-based controls, energy management schemes, or diagnosis possibilities. This paper focuses on the online estimation of the model parameters. Losses are considered in the model through a voltage source in series with the input of the converter and a current source in parallel of its output. Both the classical dc–dc boost converter and the CFDB dc–dc converter have been considered to validate the proposed modeling and estimation method. Still, the proposed modeling approach and the estimation through the proposed state observer can easily been adapted to other dc–dc converters. Simulations and experiments show the interest of the proposed state observer with better performances compared with a Luenberger state observer and an EKF especially for strongly nonlinear systems.

References

[1] E. Jamshidpour, B. Nahid-Mobarakeh, P. Poure, S. Pierfederici, F. Maybody-Tabar, and S. Saadate, "Distributed active resonance suppression in hybrid dc power systems under unbalanced load conditions," *IEEE Trans. Power Electron.*, vol. 28, no. 4, pp. 1836–1842, Apr. 2013.

[2] H. Renaudineau, "Hybrid renewable energy sourced system—Energy management & self-diagnosis," Ph.D. dissertation, Groupe de Recherche

en lectrotechnique et lectronique, Univ. Lorraine, Nancy, France, Oct. 2013.
[3] H. Barnklau, A. Gensior, and J. Rudolph, "A model-based control scheme for modular multilevel converters," *IEEE Trans. Ind. Electron.*, vol. 60, no. 12, pp. 5359–5375, Dec. 2013.
[4] R. Priewasser, M. Agostinelli, C. Unterrieder, S. Marsili, and M. Huemer, "Modeling, control, and implementation of dc-dc converters for variable frequency operation," *IEEE Trans. Power Electron.*, vol. 29, no. 1, pp. 287–301, Jan. 2014.
[5] P. Karamanakos, T. Geyer, and S. Manias, "Direct voltage control of dc-dc boost converters using enumeration-based model predictive control," *IEEE Trans. Power Electron.*, vol. 29, no. 2, pp. 968–978, Feb. 2014.
[6] A. Gensior, O. Woywode, J. Rudolph, and H. Guldner, "On differential flatness, trajectory planning, observers, and stabilization for dc-dc converters," *IEEE Trans. Circuits Syst. I, Reg. Papers*, vol. 53, no. 9, pp. 2000–2010, Sep. 2006.
[7] H. Renaudineau, A. Houari, A. Shahin, J.-P. Martin, S. Pierfederici, F. Meibody-Tabar, and B. Gerardin, "Efficiency optimization through current-sharing for paralleled dc-dc boost converters with parameter estimation," *IEEE Trans. Power Electron.*, vol. 29, no. 2, pp. 759–767, Feb. 2014.
[8] S. Shuai, P. Wheeler, J. Clare, and A. Watson, "Fault detection for modular multilevel converters based on sliding mode observer," *IEEE Trans. Power Electron.*, vol. 28, no. 11, pp. 4867–4872, Nov. 2013.
[9] T. Pavlovic, T. Bjazic, and Z. Ban, "Simplified averaged models of dcdc power converters suitable for controller design and microgrid simulation," *IEEE Trans. Power Electron.*, vol. 28, no. 7, pp. 3266–3275, Jul. 2013.
[10] Z. Zhiliang, F. Jizhen, L. Yan-Fei, and P. Sen, "Switching loss analysis considering parasitic loop inductance with current source drivers for buck converters," *IEEE Trans. Power Electron.*, vol. 26, no. 7, pp. 1815–1819, Dec. 2011.
[11] J. Linares-Flores, A. H. Mendez, C. García-Rodríguez, and H. Sira-Ramírez, "Robust nonlinear adaptive control of a boost converter via algebraic parameter identification," *IEEE Trans. Ind. Electron.*, vol. 61, no. 8, pp. 4105–4114, Aug. 2014.
[12] Y.-T. Chang and Y.-S. Lai, "Parameter tuning method for digital power converter with predictive current-mode control," *IEEE Trans. Power Electron.*, vol. 24, no. 12, pp. 2910–2919, Dec. 2009.
[13] J. Morroni, R. Zane, and D. Maksimović, "Design and implementation of an adaptive tuning system based on desired phase margin for digitally controlled dc-dc converters," *IEEE Trans. Power Electron.*, vol. 24, no. 2, pp. 559–564, Feb. 2009.
[14] A. Shahin, A. Payman, J.-P. Martin, S. Pierfederici, and F. Meibody-Tabar, "Approximate novel loss formulae estimation for optimization of power controller of dc-dc converter," in *Proc. 36th Annu. Conf. IEEE Ind. Electron. Soc.*, 2010, pp. 373–378.
[15] K. Al-Hosani and V. Utkin, "Parameters estimation using sliding mode observer with shift operator," *J. Franklin Inst.*, vol. 394, no. 4, pp. 1509–1525, May 2012.
[16] F. Auger, M. Hilairet, J. Guerrero, E. Monmasson, T. Orlowska-Kowalska, and S. Katsura, "Industrial applications of the Kalman filter: A review," *IEEE Trans. Ind. Electron.*, vol. 60, no. 12, pp. 5458–5471, Dec. 2013.
[17] A. Izadian and P. Khayyer, "Application of Kalman filters in model-based fault diagnosis of a dc-dc boost converter," in *Proc. 36th Annu. Conf. IEEE Ind. Electron. Soc.*, 2010, pp. 369–372 .
[18] O. A. Ahmed, "Investigation into high efficiency dc-dc converter topologies for a dc microgrid system," Ph.D. dissertation, Dept. Eng., Univ. Leicester, Leicester, U.K., 2011.
[19] O. Ahmed and J. Bleijs, "High-efficiency dc-dc converter for fuel cell applications: Performance and dynamic modeling," in *Proc. Energy Convers. Congr. Expo.*, 2009, pp. 67–74.
[20] L. Zhu, K. Wang, F. Lee, and J. Lai, "New start-up schemes for isolated full-bridge boost converters," *IEEE Trans. Power Electron.*, vol. 18, no. 4, pp. 946–951, Jul. 2003.
[21] B. Zhao, Q. Song, W. Liu, and Y. Sun, "Dead-time effect of the high-frequency isolated bidirectional full-bridge dc-dc converter: Comprehensive theoretical analysis and experimental verification," *IEEE Trans. Power Electron.*, vol. 29, no. 4, pp. 1667–1680, Apr. 2014.
[22] L. Zhu, "A novel soft-commutating isolated boost full-bridge ZVS-PWM dc-dc converter for bidirectional high power applications," *IEEE Trans. Power Electron.*, vol. 21, no. 2, pp. 422–429, Mar. 2006.
[23] W. Chen, "Disturbance observer based control for nonlinear systems," *IEEE/ASME Trans. Mechatronics*, vol. 9, no. 4, pp. 706–710, Dec. 2004.
[24] K. Kim and K. Rew, "Reduced order disturbance observer for discrete-time linear systems," *Automatica*, vol. 49, pp. 968–975, 2013.
[25] A. Ben-Israel and T. N. E. Greville, *Generalized Inverses—Theory and Applications*, 2nd ed. New York, NY, USA: Wiley-Interscience, 2003.
[26] S. Olteanu, A. Aitouche, L. Belkoura, and A. Nakrachi, "Robust estimation for PEM fuel cell systems," presented at the 5th Int. Conf. Fundam. Develop. Fuel Cells, Karlsruhe, Germany, 2013.

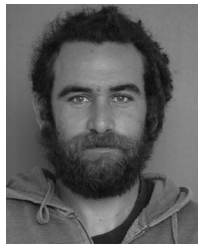

Hugues Renaudineau received the Engineer's degree from the École Nationale Supérieure d'Électricité et de Mécanique, Nancy, France, in 2009, and the Ph.D. degree from the Université de Lorraine, Nancy, in 2013.

He is currently working with the Groupe de Recherche en Électrotechnique et Électronique de Nancy, Université de Lorraine. His research interests include modeling, control, and diagnosis of photovoltaic power systems, and fault-tolerant power electronic systems.

Jean-Philippe Martin received the graduation degree from the University of Nancy, Nancy, France, and the Ph.D. degree from the Institut National Polytechnique de Lorraine (INPL), Nancy, in 2003.

Since 2004, he has been an Assistant Professor at INPL. His research interests in Groupe de Recherche en Electrotechnique et Electronique de Nancy include the stability study of distributed power system, electrical machine controls, static converter architectures, and their interactions with new electrical devices (fuel cell and photovoltaic system).

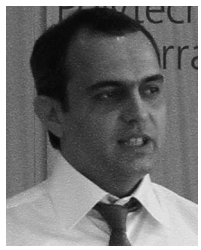

Babak Nahid-Mobarakeh (M'05–SM'12) received the Ph.D. degree in electrical engineering from the Institut National Polytechnique de Lorraine, Nancy, France, in 2001.

From 2001 to 2006, he was an Assistant Professor with the Centre de Robotique, Electrotechnique et Automatique, University of Picardie, Amiens, France. In September 2006, he joined the Ecole Nationale Superieure d'Electricite et de Mecanique, University of Lorraine, Nancy, where he is currently an Associate Professor. He is also with the Groupe de Recherche en Electrotechnique et Electronique de Nancy, Nancy. He is the author or coauthor of more than 100 international journal and conference papers. His main research interests include nonlinear and robust control techniques applied to electric systems, fault detection and fault-tolerant control of power systems, and stabilization of microgrids.

Dr. Nahid-Mobarakeh received the Best Paper Prize of the IEEE Transportation Electrification Conference in 2013 and the Second Best Paper Prize from the Industrial Automation and Control Committee of the IEEE Industry Applications Society Annual Meeting in 2010.

Serge Pierfederici received the Engineer's degree in electrical engineering from the École Nationale Supérieure d'Électricité et de Mécanique, Nancy, France, in 1994, and the Ph.D. degree from the Institut National Polytechnique de Lorraine (INPL), Nancy, in 1998.

Since 2009, he has been a Professor at INPL. His research interests include the stability study of distributed power system and the control of multisource, multiload systems.